CCNE1 and *PLK1* Mediate Resistance to Palbociclib in HR+/HER2− Metastatic Breast Cancer

Ángel Guerrero-Zotano[1,2], Stefania Belli[3], Christoph Zielinski[4,5], Miguel Gil-Gil[2,6,7], Antonio Fernandez-Serra[8], Manuel Ruiz-Borrego[2,9], Eva Maria Ciruelos Gil[2,10,11,12], Javier Pascual[2,13,14,15], Montserrat Muñoz-Mateu[2,16,17], Begoña Bermejo[2,15,18,19], Mireia Margeli Vila[2,20], Antonio Antón[2,15,21], Laura Murillo[2,22], Bella Nissenbaum[23], Yuan Liu[24], Jesús Herranz[2], Daniel Fernández-García[2], Rosalía Caballero[2], José Antonio López-Guerrero[8,25,26], Roberto Bianco[3], Luigi Formisano[3], Nicholas Turner[14], and Miguel Martín[2,15,27]

ABSTRACT

Purpose: In hormone receptor–positive (HR+)/HER2− metastatic breast cancer (MBC), it is imperative to identify patients who respond poorly to cyclin-dependent kinase 4/6 inhibitors (CDK4/6i) and to discover therapeutic targets to reverse this resistance. Non-luminal breast cancer subtype and high levels of *CCNE1* are candidate biomarkers in this setting, but further validation is needed.

Experimental Design: We performed mRNA gene expression profiling and correlation with progression-free survival (PFS) on 455 tumor samples included in the phase III PEARL study, which assigned patients with HR+/HER2− MBC to receive palbociclib+endocrine therapy (ET) versus capecitabine. Estrogen receptor–positive (ER+)/HER2− breast cancer cell lines were used to generate and characterize resistance to palbociclib+ET.

Results: Non-luminal subtype was more prevalent in metastatic (14%) than in primary tumor samples (4%). Patients with non-luminal tumors had median PFS of 2.4 months with palbociclib+ET and 9.3 months with capecitabine; HR 4.16, adjusted P value < 0.0001. Tumors with high *CCNE1* expression (above median) also had worse median PFS with palbociclib+ET (6.2 months) than with capecitabine (9.3 months); HR 1.55, adjusted P value = 0.0036. In patients refractory to palbociclib+ET (PFS in the lower quartile), we found higher levels of Polo-like kinase 1 (PLK1). In an independent data set (PALOMA3), tumors with high *PLK1* show worse median PFS than those with low *PLK1* expression under palbociclib+ET treatment. In ER+/HER2− cell line models, we show that PLK1 inhibition reverses resistance to palbociclib+ET.

Conclusions: We confirm the association of non-luminal subtype and *CCNE1* with resistance to CDK4/6i+ET in HR+ MBC. High levels of *PLK1* mRNA identify patients with poor response to palbociclib, suggesting PLK1 could also play a role in the setting of resistance to CDK4/6i.

Introduction

The cyclin D1–cyclin-dependent kinase 4/6 (CDK4/6)–RB1 axis is the major mediator of cellular proliferation mediated by estrogen signaling in estrogen receptor–positive (ER+) breast cancer. Pivotal studies of the three approved CDK4/6 inhibitors (CDK4/6i), palbociclib, ribociclib, and abemaciclib, established its combination plus endocrine therapy (ET) as the preferred first-line treatment approach for most patients with hormone receptor–positive (HR+)/HER2− metastatic breast cancer (MBC; refs. 1, 2). ET plus CDK4/6i is also an effective treatment option in second and subsequent lines of therapy, however, the absolute benefit is considerably less, and some

[1]Medical Oncology, Instituto Valenciano de Oncología, Valencia, Spain. [2]GEICAM Spanish Breast Cancer Group, Madrid, Spain. [3]Department of Clinical Medicine and Surgery, University of Naples "Federico II", Naples, Italy. [4]Medical Oncology, Central European Cancer Center, Wiener Privatklinik Hospital, Vienna, Austria. [5]CECOG Central European Cooperative Oncology Group, Vienna, Austria. [6]Institut Català d'Oncologia (ICO), Barcelona, Spain. [7]IDIBELL, L'Hospitalet, Barcelona, Spain. [8]Laboratory of Molecular Biology, Fundación Instituto Valenciano de Oncología, Valencia, Spain. [9]Medical Oncology, Hospital Universitario Virgen del Rocio, Sevilla, Spain. [10]Medical Oncology, Hospital Universitario 12 de Octubre, Madrid, Spain. [11]Medical Oncology, HM Hospitales Madrid, Madrid, Spain. [12]SOLTI Group on Breast Cancer Research, Barcelona, Spain. [13]Medical Oncology Intercenter Unit, Regional and Virgen de la Victoria University Hospitals, IBIMA, Málaga, Spain. [14]Institute of Cancer Research and Royal Marsden, London, United Kingdom. [15]Oncology Biomedical Research National Network (CIBERONC-ISCIII), Madrid, Spain. [16]Medical Oncology, Hospital Clinic de Barcelona, Barcelona, Spain. [17]Translational Genomics and Targeted Therapeutics in Solid Tumors (IDIBAPS), Barcelona, Spain. [18]Medical Oncology, Hospital Clínico Universitario de Valencia, Medicine Department, Universidad Medicina Valencia, Valencia, Spain. [19]Biomedical Research Institute INCLIVA, Valencia, Spain. [20]B-ARGO Group, Catalan Institute of Oncology- Badalona, Hospital Universitari Germans Trias i Pujol, Badalona, Spain. [21]Medical Oncology, Hospital Universitario Miguel Servet, Instituto de Investigación Sanitaria Aragón, Zaragoza, Spain. [22]Medical Oncology, Hospital Clínico de Zaragoza Lozano Blesa, Zaragoza, Spain. [23]Meir Medical Center, Kfar Saba, Israel. [24]Pfizer, La Jolla, California. [25]IVO-CIPF Joint Research Unit of Cancer, Príncipe Felipe Research Center (CIPF), Valencia, Spain. [26]Department of Pathology, School of Medicine, Catholic University of Valencia "San Vicente Mártir", Valencia, Spain. [27]Medical Oncology, Instituto de Investigación Sanitaria Gregorio Marañón, Medicine Department, Universidad Complutense, Madrid, Spain.

Á. Guerrero-Zotano and S. Belli contributed equally to this article.

ClinicalTrials.gov: NCT02028507

Corresponding Author: Miguel Martín, Medical Oncology, Instituto de Investigación Sanitaria Gregorio Marañón, CIBERONC-ISCIII GEICAM Spanish Breast Cancer Group, Madrid, Spain. Phone: 916-592-870; E-mail: mmartin@geicam.org

Clin Cancer Res 2023;XX:XX–XX

doi: 10.1158/1078-0432.CCR-22-2206

Translational Relevance

Most patients with HR+/HER2− advanced breast cancer benefit from the combination of cyclin-dependent kinase 4/6 inhibitors (CDK4/6i) and endocrine therapy (ET), but resistance invariably evolves, including patients with rapid progression. We confirm here the previously reported association of non-luminal breast cancer subtype and high *CCNE1* expression with resistance to CDK4/6i. We show that tumors expressing these biomarkers benefit more from chemotherapy (capecitabine) than from palbociclib+ET. Also, we observed that Polo-like kinase 1 (*PLK1*) mRNA levels are significantly higher in cases with the poorest response to palbociclib+ET. *In vitro* studies confirm the role of *PLK1* in driving resistance to CDK4/6i and the potential therapeutic role of PLK1 inhibition to reverse this resistance.

patients show refractory disease (3–5). No predictive biomarkers of the benefit of CDK4/6i have been identified in randomized trials. Increasing data suggest that non-luminal breast cancer subtypes and high levels of *CCNE1* are biomarkers that identify patients who derive poor absolute improvement in progression-free survival (PFS) from treatment with CDK4/6i (6–8), raising the hypothesis that these tumors might benefit from alternatives therapies. Identification of predictive biomarkers would help to distinguish patients, refractory to ET plus CDK4/6i, that might miss therapeutics opportunities, as well as to establish a rationale for alternative treatment approaches. We present here a biomarker study, using gene expression analysis of tumor tissues from the randomized controlled PEARL study that compared palbociclib plus ET versus capecitabine.

Materials and Methods

PEARL study design

The details of the PEARL study (ClinicalTrials.gov: NCT02028507) have been previously published (9). Briefly, PEARL study had two consecutive cohorts and randomly assigned 601 postmenopausal women with HR+/HER2− MBC resistant to previous aromatase inhibitors (defined as recurrence while on or within 12 months after the end of adjuvant treatment or progression while on or within 1 month after the end of treatment for advanced disease) to receive palbociclib plus ET (exemestane or fulvestrant) or capecitabine. The study hypothesized that palbociclib plus ET would be superior in term of PFS to capecitabine with a HR of 0.6. The PEARL trial was unable to show any PFS benefit from palbociclib plus ET versus capecitabine.

Research protocol was approved by every site's institutional review board and every country's regulatory agency. Studies were conducted in accordance with the Declaration of Helsinki ethical guidelines. All the patients signed written informed consents. Formalin fixed, paraffin-embedded (FFPE) tumor samples were collected prior to the study entry, when available, either from metastatic disease or from an archival primary sample for biomarker analysis.

Gene expression analysis

The EdgeSeq Oncology BM Panel (HTG Molecular Diagnostics, Tucson, AZ) was used for mRNA profiling of 2,549 transcripts of cancer genes. This system uses targeted capture sequencing to quantitate RNA expression levels of gene targets in tissues, followed by a standard RNA sequencing protocol in a Next-Generation Sequencer. Sample preparation was conducted by following the laboratory process and manufacturer protocols. Sequencing was performed on a NextSeq 500 sequencer (Illumina, San Diego, CA). Gene expression data were quantile normalized and log2 transformed. Raw data are deposited in the Gene Expression Omnibus (National Center for Biotechnology Information – National Institutes of Health, NCBI-NIH, Bethesda, MD).

Molecular subtype classification

Intrinsic subtype assignment was performed using AIMS package (2). This method implements naïve Bayes classifier composed of the 100 rules described to assign between five groups in breast cancer samples [Luminal A (LumA), Luminal B (LumB), HER2-enriched, Basal-like and Normal-like]. Because Normal-like subtype is usually indicative of low cellularity, we decided to exclude Normal-like samples for further analysis. Normalization and pre-visualization of the results was performed with R v3.6.1.

Statistical analysis

A within-treatment arm Cox proportional hazards regression analysis followed by a cross arm gene-treatment interaction analysis was performed to investigate potential interactions between gene expression levels, as a continuous variable, and treatment effects in terms of PFS. Interaction *P* values were adjusted using the Benjamini-Hochberg FDR. Genes resulting from this analysis were studied by a gene set enrichment analysis (GSEA) using MsigDB Hallmarks of cancer (10). To investigate genes differentially expressed in extreme responders to palbociclib plus ET, samples were subset in 2 categories: (i) refractory, PFS in the lower quartile, and (ii) sensitive, PFS within the upper quartile. We performed a differential gene expression analysis between the two groups using Significance Analysis of Microarrays (SAM) method and adjusting for multiple comparisons. Multivariate Cox regression analysis for selected genes of this analysis was performed, accounting for prognostic variables (age, site of disease, sites of metastasis, prior chemotherapy for MBC, Ki67) and by treatment interaction.

Cell lines and inhibitors

MCF-7 (ATCC HTB-22), T47D (ATCC HTB-133) human breast cancer cells were obtained from the ATCC (Manassas, VA) and maintained in ATCC-recommended media supplemented with 10% FBS (Gibco, Waltham, MA) and 1× antibiotic/antimycotic (Gibco). MCF7-PalboR, MCF7-FPR, T47D-PalboR, and T47D-FPR cells were generated after 6 months of treatment with increasing doses of palbociclib alone (PalboR cells) or in combination with fulvestrant (FPR cells), up to 1 μmol/L final concentration. MCF7-CTRL and T47D-CTRL were obtained after lentiviral infection with pLenti-C-mGFP control (OriGene). Likewise, MCF7-PLK1 and T47D-PLK1 were generated after lentiviral infection with mGFP-tagged-PLK1 pLenti-ORF clone particles, stable overexpressing full lenght mGFP-tagged-PLK1 kinase, as described later. All experiments were performed < 2 months after thawing early passage cells. Mycoplasma testing was conducted for each cell line before use.

Fulvestrant, palbociclib, and volasertib were purchased from SelleckChem (Houston, TX) for this preclinical work.

Cell viability assays

Cells (5×10^3/well) were seeded in triplicate in DMEM 10% FBS (ThermoFisher Scientific) in 96-well plates and treated with the indicated drugs. Media drugs were replenished every 3 days until

control wells reached 50% to 70% confluency. Monolayers were then fixed and stained with 20% methanol/80% water/0.25% crystal violet for 20 minutes, washed with water, and dried. Stained cells were solubilized with 20% acid acetic solution, and the absorbance was measured by spectrophotometric detection at 490 nm using a plate reader (GloMax Discover Microplate Reader; Promega, Madison, WI). Drug synergism and combination indices were determined using the Chou-Talalay test by CompuSyn software.

RT-PCR, qPCR

RNA was isolated using TRIzol and 1 μg of RNA/sample was reverse-transcribed using SuperScript III Reverse Transcriptase (Invitrogen), according to the manufacturer's instructions. Quantitative PCRs (qPCR) were performed on the CFX Connect Real-Time PCR Detection System (Bio-Rad), using iTaq Universal SYBR Green Supermix (Bio-Rad). GAPDH gene was used as reference for data normalization and relative gene expression was measured with the $2^{-\Delta\Delta Ct}$ method.

qPCR oligo PAIRS for *PLK1* gene were: 5′-CCTGCACCGAAACCGAGTTA-3′ (Fwd) and 5′-TAGGAGTCCCACACAGGGTC-3′ (Rev).

Western blot

Cells were lysed with RIPA lysis buffer (sc-24948, Santa Cruz Biotechnology, Inc., Dallas, TX) according to the protocol supplied. Whole cell lysates (30 μg) were separated by SDS-PAGE, transferred to nitrocellulose through Trans-Blot Turbo RTA Mini Nitrocellulose Transfer Kit (Bio-Rad, Hercules, CA, USA). Membranes were subjected to immunoblot analyses using primary antibodies against phosphorylated RB (Ser780) #8180 1:1,000 (Cell Signaling Technology, Danvers, MA), phosphorylated RB (Ser807/811) #8516 1:1,000 (Cell Signaling Technology), RB (IF-8) #sc102 1:1,000 (Santa Cruz Biotechnology, Inc.), Erα (F-10) #sc-8002 1:200 (Santa Cruz Biotechnology, Inc.), PLK1 (208G4) #4513 (Cell Signaling Technology) 1:1,000, β-actin (13E5) rabbit mAb #4970 (Cell Signaling Technology) 1:5,000, PARP (46d11) rabbit mAb #9532 (Cell Signaling Technology), GAPDH #sc-32233 1:10,000 (Santa Cruz Biotechnology, Inc.), HRP-conjugated anti-rabbit and anti-mouse were used as secondary antibodies (Bio-Rad). Immunoreactive proteins were visualized by enhanced chemiluminescence using SuperSignal West Pico PLUS Chemiluminescent Substrate (Thermo Fisher Scientific, Waltham, MA). Membranes were cut horizontally to probe with multiple antibodies. Films were imaged using Brother MFCL2710DW (Brother) at 300 dpi.

Breast cancer spheroids assay

Cells were seeded in Ultra-Low attachment 96 plate (Corning, Inc., Corning, NY), in quadruple assays, using 100 μL of 10% DMEM-FBS for 48 hours. For cell lines MCF7, MCF7-PalboR, MCF7-CTRL, MCF7-PLK1, MCF7-FPR, 5×10^3 cells were seeded, and 10×10^3 cells for T47D, T47D-PalboR, T47D-CTRL, T47D-PLK1, T47D-FPR cell lines. After representative images were captured at Invitrogen EVOS FL imaging system (20X magnification; Invitrogen, Waltham, MA), spheroids were treated for 72 hours as detailed in the specific figure legends. Tumor spheroids growth was monitored at the inverted microscope, the area was quantified with the ImageJ 1.53 software (NIH, Bethesda, MD) and normalized to time 0 area. Spheroids from MCF7 or T47D parental, PalboR or FPR transfected with siCTRL or siPLK1 were set up after 48 hours from the transfection. Then, they were treated and the area was measured as described in the figure legends.

siRNA transfections

Cells were transfected using Lipofectamine RNAi-MAX (Invitrogen, Waltham, MA) and 40 nmol/L siRNA (Scrambled Negative Control DsiRNA—IDT, catalog no. 229044958) or a pool of 3 different DsiRNA against *PLK1* mRNA: hs.Ri.PLK1.13.1 #226000069, hs.Ri.PLK1.13.2 #226000066, hs.Ri.PLK1.13.3 #226000063 (IDT) at 40 nmol/L final concentration. After 2 days, cells were seeded in 10% DMEM-FBS in either ultra-low attachment 96-well plates (5×10^3/well for proliferation assays) or in 60-mm plates (for immunoblot analysis) and treated at the indicated drug concentrations for 72 hours. For immunoblot analyses, the cells were harvested and protein lysates prepared 3 days after transfection and 3 more days after drug treatment. Representative images of tumor spheroids were captured at Invitrogen EVOS FL imaging system (20X magnification) the day after seeding and 6 days after drug treatment (media ± drug were changed every 72 hours).

Viral transduction

Human mGFP-tagged-PLK1 (RC201795L4V) and pLenti-C-mGFP-P2A-Puro control (PS100071V) lenti-ORF clone particles were purchased from OriGene. To generate stably transduced lines, 25 μL of lenti-ORF particles were transfected with 8 μg/mL polybrene (Sigma-Aldrich, Merck, KGaA, Darmstadt, Germany) in MCF7 and T47D parental cells. After 48 hours, transduced cells were selected in 1 μg/mL puromycin.

Data availability

The biological data that originated this study has been uploaded into GEO DataSets, a publicly accessible data repository. Access the information on GEO DataSets using the accession number GSE223700.

The clinical database of this study is available from the corresponding author on reasonable request.

Results

Characteristics and treatment efficacy in the biomarker study cohort and whole PEARL cohort

The biomarker cohort included 455 patients out of the 601 (75.7%) total patients randomized in the trial with an archival FFPE tumor sample available for biomarker analysis (72% primary, 27% metastatic and 1% unknown). Of them, 229 patients were from the palbociclib plus ET arm (50.3%) and 226 from the capecitabine arm (49.7%; Supplementary Fig. S1). Baseline clinical and pathologic characteristics and PFS were similar between the biomarker cohort and whole PEARL study cohort (Supplementary Fig. S2). This comparison allows us to validate the biomarker cohort for analysis and provide us with enough evidence to consider the biomarker cohort as representative of the whole PEARL study cohort.

Non-luminal intrinsic subtype is associated with resistance to palbociclib plus ET but not to capecitabine

We explored the interaction between intrinsic subtypes and treatment benefit in the biomarker cohort. The breast cancer intrinsic subtypes were assigned using the single sample predictor algorithm Absolute Intrinsic Molecular Subtyping (AIMS) classifier, via EdgeSeq Oncology BM Panel (HTG Molecular Diagnostics) for genomic expression mRNA profiling. The AIMS-HTG intrinsic subtypes distribution was 51.0% LumA, 42.2% LumB, 6.4% HER2-enriched, and 0.4% Basal-like. There was a higher proportion of non-luminal subtypes in metastatic (14%) than in

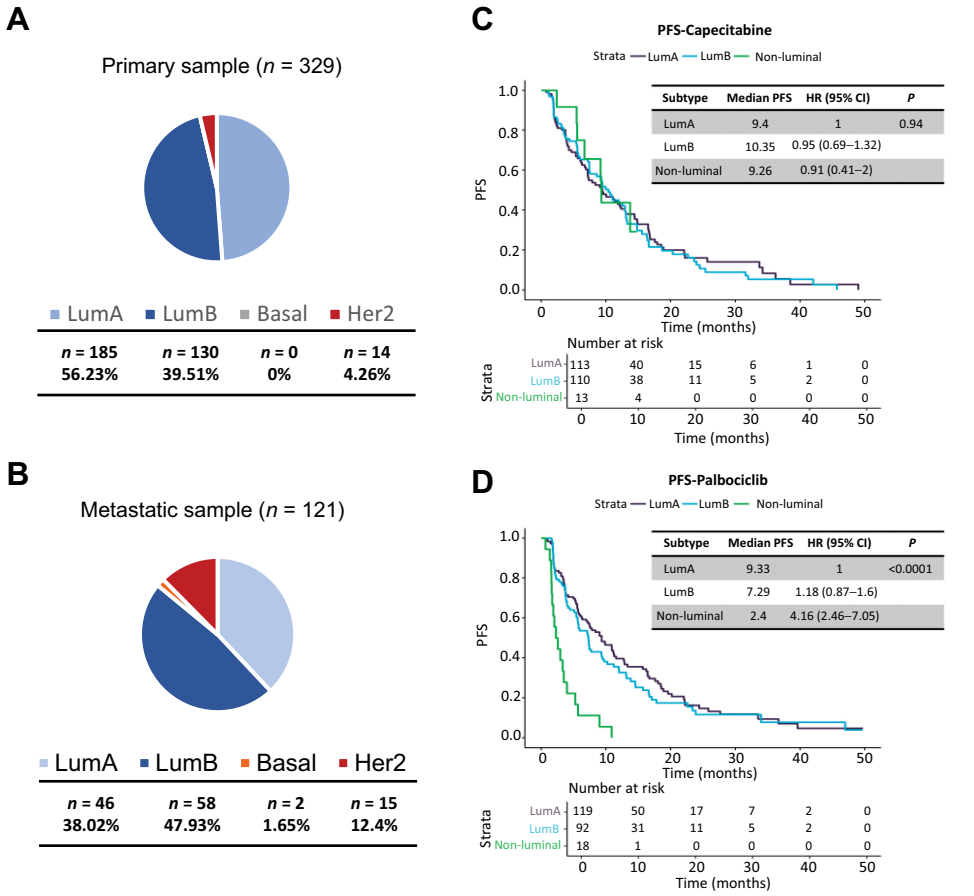

Figure 1.
Non-luminal AIMS-HTG intrinsic subtype is associated with resistance to palbociclib but not to capecitabine. **A,** Intrinsic subtype distribution in patients with AIMS-HTG performed in primary tumor samples or (**B**) in metastatic tumor samples. **C,** PFS according to AIMS-HTG intrinsic subtypes in patients treated with capecitabine or (**D**) with palbociclib plus ET. In PFS curves, Kaplan–Meier plots are used to represent the survival curves, while Cox models, adjusted by prognosis variables, are used to represent the values.

primary samples (4%; *P* value = 0.0006; **Fig. 1A** and **B**). Patients with Luminal tumors showed a median PFS of 9.3 and 7.3 months (LumA and LumB, respectively) with palbociclib plus ET ($n = 211$, 92.14%), and 9.4 and 10.3 months with capecitabine ($n = 213$, 94.25%). Patients with non-luminal tumors had a median PFS of 2.4 and 9.3 months with palbociclib plus ET ($n = 18$, 7.86%) and capecitabine ($n = 13$, 5.75%), respectively (**Fig. 1C** and **D**). After adjusting for prognostic variables, the association between PFS and subtype was statistically significant for palbociclib plus ET arm [LumA as reference, Lum B (adjusted HR, 1.18; 95% confidence interval (CI), 0.87–1.6) and non-luminal (adjusted HR, 4.16; 95% CI, 2.46–7.05); *P* value < 0.0001] but not for capecitabine arm [LumA as reference, Lum B (adjusted HR, 0.95; 95% CI, 0.69–1.32) and non-luminal (adjusted HR, 0.91; 95% CI, 0.41–2); *P* value = 0.94; **Fig. 1C** and **D**]. The interaction analysis between treatment arm and the AIMS-HTG intrinsic subtypes was significant (adjusted *P* value < 0.00013). This interaction between intrinsic subtypes and treatment benefit was maintained regardless of the source of tumor tissue analyzed (primary or metastatic sample; Supplementary Fig. S3).

CCNE1 mRNA expression is increased in metastases and associated with resistance to palbociclib plus ET

We explored *CCNE1* mRNA expression as predictive biomarker of treatment efficacy. Median *CCNE1* was higher in metastatic than in primary tumors (7.28 vs. 6.89, *P* value = 0.004) and in LumB and non-luminal subtypes compared with LumA (7.29 and 7.94 vs. 6.52; *P* value < 0.0001; **Fig. 2A** and **B**). In 14 patients with paired primary and metastatic tumor samples available, median *CCNE1* expression was higher in the metastases than in the primary tumors, although not statistically significant (7.18 vs. 6.34, *P* value = 0.07; **Fig. 2C** and **D**).

In tumors with high *CCNE1* expression (above the median), median PFS was 6.21 months on palbociclib plus ET and 9.26 months on capecitabine, while in tumors with low *CCNE1* expression (below the median), median PFS was 9.43 months on palbociclib plus ET and 10.84 months on capecitabine. After adjusting for prognostic variables, the association between PFS and *CCNE1* expression levels was significant for palbociclib plus ET (adjusted HR = 1.55; 95% CI, 1.15–2.08; *P* value = 0.0036), but not for capecitabine (adjusted HR = 1.01; 95% CI, 0.74–1.38; *P* value = 0.957; **Fig. 2E** and **F**). The Interaction analysis between treatment arm and *CCNE1* was significant (adjusted *P* value = 0.031). The origin of tumor biopsy, primary or metastatic, had an impact on the magnitude of benefit of palbociclib plus ET according to *CCNE1* expression. Palbociclib plus ET showed a median PFS of 8.38 months in primary tumors with low *CCNE1* expression, while in metastatic tumors with low *CCNE1* expression median PFS was of 16.4 months (Supplementary Fig. S4A and S4B). Then we assessed the impact of *CCNE1* expression on palbociclib plus ET efficacy by intrinsic subtype. LumB tumors showed a numerical trend to better PFS with low *CCNE1* (median PFS 12.02 vs. 7.06 months, HR = 1.57; 95% CI, 0.97–2.56; *P* value = 0.0631). For LumA tumors, the efficacy of palbociclib+ET was maintained regardless of *CCNE1* levels. We didn't perform this analysis in non-luminal tumors due to low sample size (Supplementary Fig. S4C and S4D).

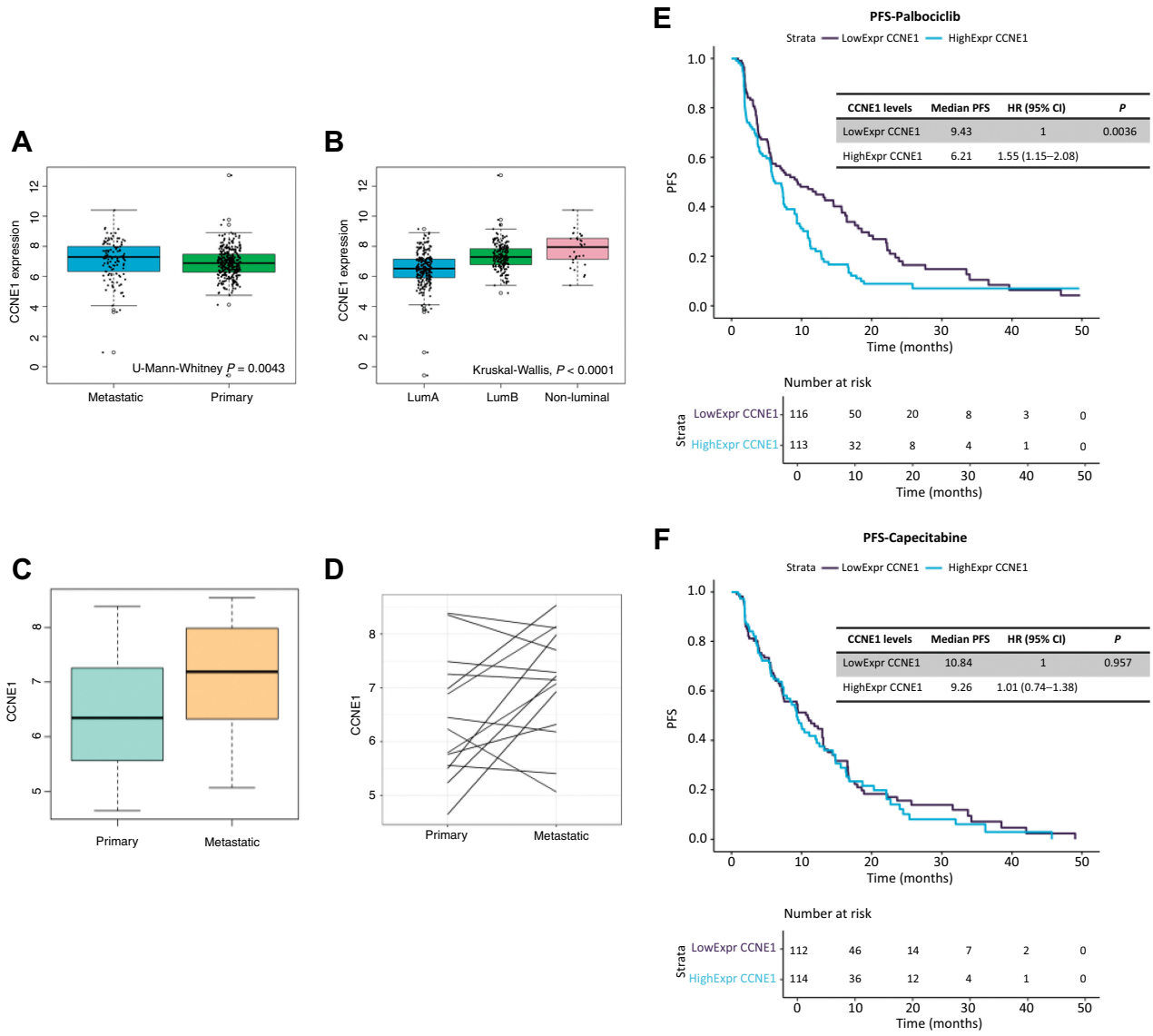

Figure 2.

CCNE1 mRNA expression is increased in metastases and associated with resistance to palbociclib plus ET. CCNE1 mRNA expression levels according to (**A**) source of tumor sample or (**B**) AIMS-HTG subtypes. **C,** Levels of CCNE1 mRNA expression in a set of 14 paired tumors (primary-metastatic). **D,** Paired individual mRNA CCNE1 expression levels in 14 paired tumors (primary-metastatic). PFS analysis according to expression levels of CCNE1 in patients treated with (**E**) palbociclib plus ET or (**F**) with capecitabine. In PFS curves, Kaplan–Meier plots are used to represent the survival curves, while Cox models, adjusted by prognosis variables, are used to represent the values. LowExpr CCNE1 (below median value); HighExpr CCNE1 (above median value); median value = 6.980949.

Discovery analysis of gene expression and its association with treatment benefit

To understand if the magnitude of the benefit, either of palbociclib plus ET or capecitabine, differs according to expression levels of any of the 2,549 genes included in the gene panel, we carried out a within-arm PFS Cox regression analysis followed by a cross-arm gene expression treatment interaction test, using gene expression as a continuous variable, and adjusting for prognostic variables. In the palbociclib plus ET arm, 17 genes were associated with PFS; whilst the interaction test showed, 11 genes associated with sensitivity and 3 genes (*CCNE1, PLK1*, and *MELK*) with resistance to palbociclib plus ET (FDR < 0.1). In the GSEA, using MsigDB Hallmarks of cancer (10), E2F_Targets was the top signature associated with resistance and Estrongen_Response_Early with sensitivity to palbociclib plus ET (Supplementary Fig. S5A and S5B).

In the capecitabine arm, 855 genes were associated with PFS; in the interaction test, 100 genes with sensitivity and 39 with resistance (FDR < 0.1). In the GSEA, P53_Pathway was the top signature associated with resistance and Inflammatory_Response with sensitivity to capecitabine (Supplementary Fig. S5C and S5D).

Clinicopathologic characteristics and gene expression profile of extreme responders to palbociclib plus ET

The poor performance of some patients treated with palbociclib plus ET urge the need to identify biomarkers of refractory tumors. We classified tumors treated with palbociclib plus ET in sensitive (PFS in

upper quartile, $n = 56$; median PFS 22.2 months) and refractory (PFS in the lower quartile, $n = 48$, median PFS: 1.8 months; **Fig. 3A**). Compared with the sensitive cohort, the cohort of refractory patients showed increased proportion of tumors with Ki67 ≥ 20% (60% vs. 35%), less proportion of LumA tumors (40% vs. 60%) and higher proportion of non-luminal tumors (19% vs. 0%). Fifty-one genes (FDR < 0.05) were differentially expressed between the two groups. Importantly, *CCNE1* was also identified by this approach as a resistance biomarker, together with other cell-cycle genes such as *PLK1* (Supplementary Table S1).

Unsupervised hierarchical clustering of all tumors treated with palbociclib plus ET ($n = 229$), based on the expression of these 51 genes, revealed two clusters: (i) Cluster 1, composed of resistant tumors, median PFS: 5.6 months, highly proliferative (Ki67 ≥ 20: 58%) with a high proportion of LumB (61%) and non-luminal tumors (12%); and (ii) Cluster 2, composed of sensitive tumors, median PFS, 10.9 months, low proliferative (Ki67 ≥ 20%: 31%), mostly LumA tumors (84%; **Fig. 3B**; Supplementary Table S2 and Supplementary Table S3). To validate this result in an independent dataset, we used gene expression data from PALOMA3 study, that use same gene expression platform (HTG) and same method for intrinsic subtyping assignment (AIMS). K-means clustering of the patients in the palbociclib+fulvestrant arm based, on the expression of the 51 genes associated with resistance to palbociclib in our study, revealed two clusters: (i) Cluster 1, with high proportion of LumB tumors (50%), 21% of non-luminal tumors; and median PFS 9.4 months; and (ii) Cluster 2, with a high proportion of LumA tumors (57%), 24% of non-luminal tumors and median PFS 14.06 months. Ki67 data was not available in PALOMA3 (Supplementary Fig. S6A and S6B).

High levels of *PLK1* are associated with poor response to palbociclib plus ET

Among the differentially expressed genes associated with tumors refractory to palbociclib plus ET we decided to focus on *PLK1*, as a recognized target for cancer therapy, with treatment options available, and known to be related to ER+ breast cancer treatment resistance. Like *CCNE1*, median *PLK1* was higher in metastatic than in primary tumors (8.59 vs. 8.33; P value = 0.023) and in LumB and non-luminal subtypes compared with LumA (8.87 and 9.11 vs. 7.93; P value < 0.0001; **Fig. 3C**). *PLK1* and *CCNE1* mRNA expression were moderately correlated (Pearson correlation coefficient: 0.488; 0.474 in Luminal tumors -LumA+LumB-, and 0.287 in non-luminal tumors; figures by subtype not shown), and clustered in proximity in a clustered correlation matrix using expression values of the 51 differentially expressed genes between extreme responders to palbociclib plus ET (**Fig. 3D** and **E**). Patients with high levels (above the median) of *PLK1* (*PLK1*-high) treated with palbociclib plus ET, had a worse PFS, in a multivariate model, than *PLK1*-low (5.68 vs. 9.33 months; adjusted HR = 1.64; 95% CI, 1.22–2.22; P value = 0.0012). There were no differences according to *PLK1* expression levels in patients treated with capecitabine (10.35 vs. 9.4 months, *PLK1*-High vs. -Low; adjusted HR = 0.89; 95% CI, 0.65–1.21; P value = 0.4535; **Fig. 3F** and **G**).

Finally, in a multivariate analysis of PFS in patients treated with palbociclib plus ET, and including tumor subtype, *CCNE1* and *PLK1*; high levels of *PLK1* (HR, 1.43; P value, 0.047) and non-luminal subtype (HR, 3.0; P value, 0.0001) remained statistically associated with worst PFS, while high *CCNE1* was marginally associated (HR, 1.35; P value, 0.056).

Confirmatory analysis to validate the association of *PLK1* with resistance to CDK4/6 were assayed in a different dataset, such as PALOMA3. This validation analysis confirms, in the palbociclib treatment arm, that patients with *PLK1* high expression levels show a worse median PFS than those with *PLK1* low expression levels (9.53 vs. 13.53 months; Supplementary Fig. S6C).

Fulvestrant and palbociclib–resistant ER±/HER2− breast cancer cell lines express higher PLK1 levels compared with sensitive parental cells under pharmacologic treatment

To assess the role of *PLK1* as mediator of resistance to CDK4/6i, we generated two ER+/HER2− breast cancer cells line models (MCF7 and T47D) resistant to palbociclib (PalboR) or to the combination of fulvestrant plus palbociclib (FPR). Breast tumor spheroids from both MCF7-FPR and T47D-FPR showed the ability to grow in presence of fulvestrant and palbociclib alone or in combination, compared with tumor spheroids from parental cells (**Fig. 4A**; Supplementary Fig. S7A–S7C). Moreover, even if PalboR cells were not exposed to fulvestrant, both T47D-PalboR and MCF7-PalboR resulted cross-resistant also to ER down-regulator (**Fig. 4A**; Supplementary Fig. S7A–S7C).

Gene expression analysis showed that *PLK1* mRNA was strongly downregulated upon palbociclib or fulvestrant + palbociclib treatment after 24, 48, and 72 hours in both T47D and MCF7 (Supplementary Fig. S7D and S7E). On the contrary, T47D-PalboR or -FPR and MCF7-PalboR or -FPR resistant cells showed significantly higher *PLK1* mRNA levels compared with the respective parental cell lines, in presence of pharmacologic treatment even after 72 hours (Supplementary Fig. S7D and S7E).

In accordance with *PLK1* mRNA analysis, PLK1 protein levels were completely abrogated after treatment with palbociclib alone or in combination with fulvestrant in both parental MCF7 and T47D cells, while PalboR and FPR cells maintained higher PLK1 protein levels after pharmacologic treatment (**Fig. 4B**; Supplementary Fig. S7F, respectively). Also, MCF7 and T47D cells treated with palbociclib alone or in combination with fulvestrant, showed a strong decrease of CDK4/6i and ET targets (phosphorylated – Rb, at both Ser780 and Ser807/811, ER-α and PLK1). Both PalboR and FPR cells showed lower ER-α protein levels compared with respective parental cells, whose levels further decreased upon palbociclib and fulvestrant treatment. Palbociclib strongly affected also phosphorylated – Rb protein levels in PalboR cells in both MCF7 and T47D, but not in T47D-FPR cells (**Fig. 4B**; Supplementary Fig. S7F). Interestingly, unlike T47D-FPR, MCF7-FPR cells showed the loss of both phosphorylated and total Rb protein levels, which according to previous observations is one of the main causes of resistance to CDK4/6i (i.e., palbociclib; **Fig. 4B**).

PLK1 expression regulates the response to ET and CDK4/6i in ER± breast cancer cell lines

We hypothesized that PLK1 kinase might play a role in the mechanisms of resistance to ET plus CDK4/6i (i.e., fulvestrant plus palbociclib) in ER+ breast cancer models. Hence, we verified the effects of *PLK1* gene modulation by transfecting MCF7 and T47D (parental and resistant) cells with siRNA against PLK1, achieving after 24 hours a significant reduction of *PLK1* mRNA and protein expression in all cell lines (Supplementary Fig. S8A–S8D). *PLK1* silencing significantly reduced tumor spheroid formation in MCF7 and T47D cells resistant to palbociclib or to fulvestrant+palbociclib (**Fig. 4C**; Supplementary Fig. S8E and S8F). The degree of tumor growth inhibition was greater when *PLK1* silencing was combined with fulvestrant and palbociclib. Interestingly, in parental cells, *PLK1* silencing had only a partial effect on tumor growth (**Fig. 4C**; Supplementary Fig. S8E and S8F). Next, we tested if high levels of *PLK1* could abrogate the sensitivity of parental cells to fulvestrant and palbociclib.

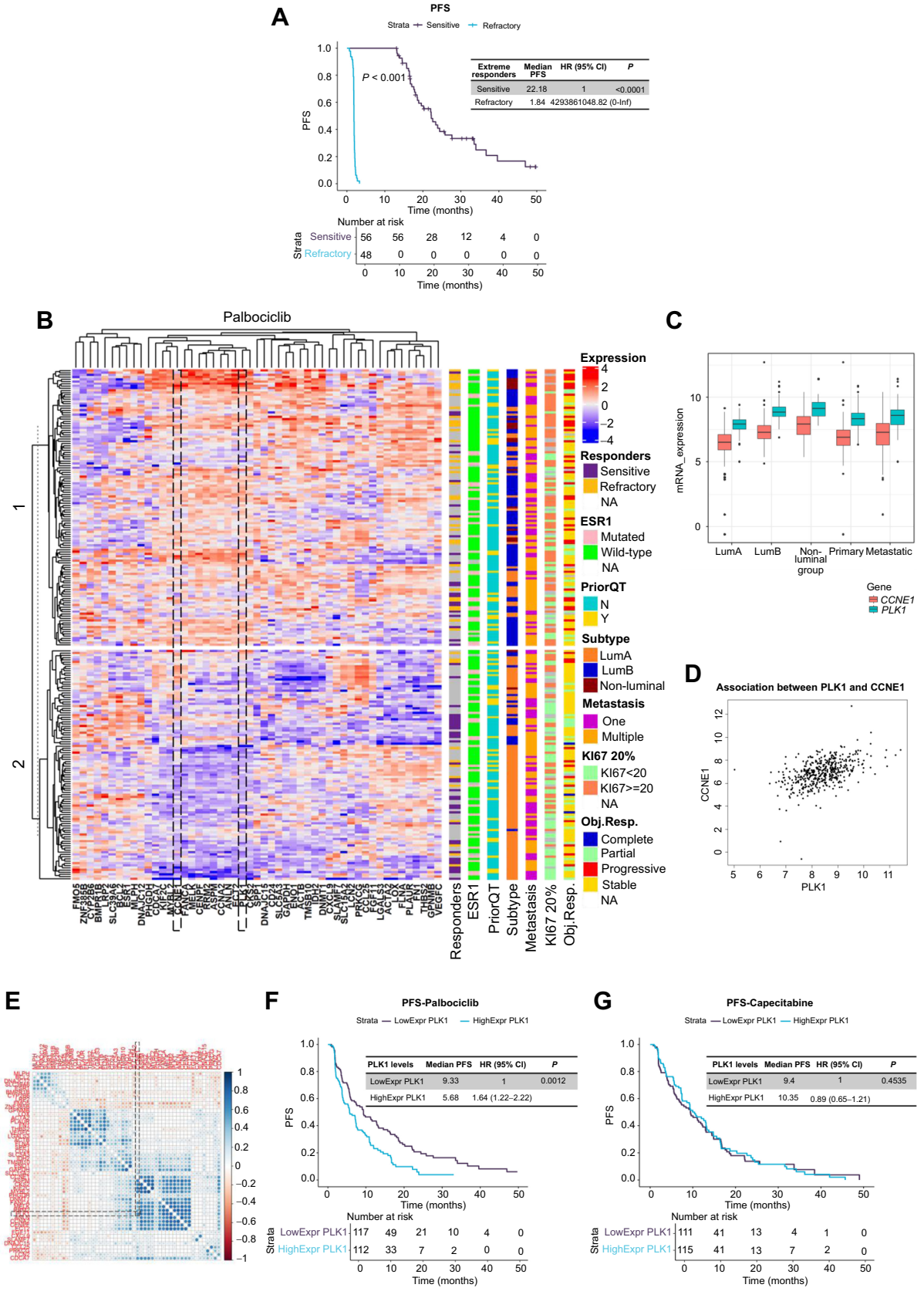
A
PFS
Strata Sensitive Refractory
P < 0.001
Extreme responders | Median PFS | HR (95% CI) | P
Sensitive | 22.18 | 1 | <0.0001
Refractory | 1.84 | 4293861048.82 (0-Inf)
PFS
Time (months)
Number at risk
Strata
Sensitive 56 56 28 12 4 0
Refractory 48 0 0 0 0 0
B
Palbociclib
Expression
Responders
Sensitive
Refractory
NA
ESR1
Mutated
Wild-type
NA
PriorQT
N
Y
Subtype
LumA
LumB
Non-luminal
Metastasis
One
Multiple
KI67 20%
KI67<20
KI67>=20
NA
Obj.Resp.
Complete
Partial
Progressive
Stable
NA
C
mRNA_expression
LumA LumB Non-luminal group Primary Metastatic
Gene
CCNE1
PLK1
D
Association between PLK1 and CCNE1
CCNE1
PLK1
E
F
PFS-Palbociclib
Strata LowExpr PLK1 HighExpr PLK1
PLK1 levels | Median PFS | HR (95% CI) | P
LowExpr PLK1 | 9.33 | 1 | 0.0012
HighExpr PLK1 | 5.68 | 1.64 (1.22–2.22)
Number at risk
LowExpr PLK1 117 49 21 10 4 0
HighExpr PLK1 112 33 7 2 0 0
G
PFS-Capecitabine
Strata LowExpr PLK1 HighExpr PLK1
PLK1 levels | Median PFS | HR (95% CI) | P
LowExpr PLK1 | 9.4 | 1 | 0.4535
HighExpr PLK1 | 10.35 | 0.89 (0.65–1.21)
Number at risk
LowExpr PLK1 111 41 13 4 1 0
HighExpr PLK1 115 41 13 7 2 0

To this end, we overexpressed mGFP tagged-PLK1 in parental MCF7 (MCF7-PLK1) and T47D (T47D-PLK1) cell lines through lentiviral infection. The efficiency of *PLK1* overexpression was assessed by immunoblot that showed, beyond the endogenous form, also an additional exogenous mGFP tagged-PLK1 band in MCF7 and T47D cells after lentiviral infection (Supplementary Fig. S8G). We observed, by tumor spheroids formation assay, that MCF7-PLK1 and T47D-PLK1 cell lines had decreased sensitivity to fulvestrant and palbociclib treatment (**Fig. 4D**; Supplementary Fig. S8H). Thus, these data show that ER+/HER2− breast cancer cells resistant to palbociclib plus ET maintain high levels of *PLK1* and depend on *PLK1* for tumor growth.

Volasertib (a PLK1 inhibitor) overcomes resistance to fulvestrant and palbociclib

To assess the effect of PLK1 pharmacologic inhibition in the reversion of drug resistance of PalboR or FPR cell to palbociclib alone or with fulvestrant, we tested the effects of a small inhibitor targeting ATP-binding pocket of PLK1 kinase domain, volasertib (11) on cell viability, tumor spheroid growth and apoptosis. Firstly, we evaluated drug interaction using Chou-Talalay method (12), where a combination index (CIx) < 1 indicates synergy. Viability assays using increasing concentrations of volasertib and fulvestrant and/or palbociclib demonstrated a pharmacologic synergism between these agents in both MCF7-FPR and T47D-FPR [CIx = 0.2 fulvestrant_volasertib, CIx = 0.29 palbociclib_volasertib, and CIx = 0.29 FP_volasertib in MCF7-FPR (**Fig. 5A**); CIx = 0.37 fulvestrant_volasertib, CIx = 0.32 palbociclib_volasertib, and CIx = 0.27 FP_volasertib in T47D-FPR (Supplementary Fig. S9A)]. Moreover, using lower doses of fulvestrant and/or palbociclib, drug interaction assays revealed a synergism also in MCF7 and T47D cells, but with higher combination indices [CIx = 0.72 fulvestrant vs. volasertib, CIx = 0.36 for palbociclib vs. volasertib and CIx = 0.5 for FP vs. volasertib in MCF7 (Supplementary Fig. S9B). CIx = 0.67 fulvestrant vs. volasertib, CIx = 0.44 for palbociclib vs. volasertib and CIx = 0.7 for FP vs. volasertib in T47D (Supplementary Fig. S9C)].

The combination of volasertib with palbociclib or palbociclib plus fulvestrant completely abrogated both PalboR and FPR tumor spheroid growth, respectively (**Fig. 5B** and **C** for MCF7 and Supplementary Fig. S10A and S10B for T47D). Likewise, the use of paclitaxel strongly inhibited PalboR and FPR growth, similarly to the effect of volasertib combined to palbociclib ± fulvestrant. In parental MCF7 or T47D and PalboR cells, volasertib decreased ER-α protein levels and phospho-Rb (at both Ser780 and 807/811; Supplementary Fig. S10C and S10D), whose levels resulted completely abrogated in combination with palbociclib. As described above, unlike T47D-FPR, MCF7-FPR cells showed the loss of phospho-Rb protein levels and lower ER-α protein levels compared with parental cells (Supplementary Fig. S10E and S10F). Moreover, the expression of cleaved form of PARP protein, an apoptosis marker, was found increased after treatment with volasertib alone or in combination with palbociclib in PalboR cells, or with fulvestrant plus palbociclib in FPR cells (Supplementary Fig. S10C and S10F), confirming the proapoptotic effects of volasertib previously described (13). As previously described, *PLK1*-overexpressing cells showed an increase 3D growth ability in presence of fulvestrant and palbociclib, unless exposed to volasertib, or paclitaxel (Supplementary Fig. S11A and S11C). T47D-PLK1, but not MCF7-PLK1 cells, exhibited an increase in phospho-Rb and ER-α protein levels compared with parental T47D cells (Supplementary Fig. S11D and S11E), whose levels (phospho-Rb and ER-α) strongly decreased after treatment with volasertib alone or in combination with fulvestrant and palbociclib, alongside with an increase in apoptotic markers in both MCF7-PLK1 and T47D-PLK1 models (i.e., cleaved form of PARP protein; Supplementary Fig. S11D and S11E).

Together, these data suggest that the pharmacologic inhibition of PLK1 kinase overcomes resistance to ET plus CDK4/6i and exerts a proapoptotic effect in ER+/HER2− breast cancer models with high levels of *PLK1*. Moreover, similarly to volasertib, paclitaxel also prevents cell proliferation of PalboR, FPR or *PLK1*-overexpressing cells, showing the effectiveness of chemotherapy in fulvestrant and/or palbociclib resistant or *PLK1*-overexpressing breast cancer models.

Discussion

Here, we present a biomarker study which shows that gene expression profiling could help to identify tumors deriving very limited efficacy to palbociclib plus ET and that might derive greater benefit with chemotherapy or other investigational agents such as PLK1 inhibitors.

Currently, HR+/HER2− MBC is an incurable disease in practically all patients. Commonly, the therapeutic approach for HR+/HER2− MBC has been sequential ET-based regimens until disease is endocrine resistant, then change to single-agent chemotherapy. CDK4/6i are now established as a standard of care for both endocrine-sensitive and endocrine resistant HR+/HER2− MBC. In combination with fulvestrant, CDK4/6i (palbociclib, ribociclib, abemaciclib) are approved for patients after progression to previous ET. In PALOMA-3 trial, the combination of palbociclib plus fulvestrant compared with fulvestrant monotherapy, significantly improved PFS by 5 months. However, the poor performance of fulvestrant, median PFS of just 4.6 months, prompted the hypothesis that in tumors that progressed previously to ET, a more reasonable comparator to palbociclib plus ET would be capecitabine, a widely used chemotherapy agent in the setting of HR+/HER2− MBC endocrine resistant. This rationale was tested in the PEARL study, which failed to demonstrate superiority of palbociclib

Figure 3.
Clinicopathologic and genomic characteristics of extreme responders to palbociclib plus ET. **A,** PFS analysis in extreme responder patients (sensitive vs. refractory), under palbociclib plus ET treatment. **B,** Unsupervised hierarchical clustering complete linkage and euclidean distance of $n = 229$ patients treated with palbociclib plus ET according to 51 differentially expressed significant genes by SAM analysis (FDR < 0.05), in refractory versus sensitive tumors (each row represents a patient, and each column a gene). Also includes the measure of proliferation by Ki67, as well as the clinical subtype classification of patients in LumA, LumB, and non-luminal; the presence of ESR1 mutations; the presence of one or multiple metastases; and the type of response to treatment. **C,** Boxplot showing mRNA expression levels of PLK1 and CCNE1 according to tumor subtype and source of tissue in the whole biomarker cohort (**D**). Correlation plot between mRNA expression levels of PLK1 and CCNE1 in the whole biomarker cohort. **E,** Correlation matrix and unsupervised hierarchical clustering (complete linkage and euclidean distance of the 51 differentially expressed genes in refractory versus sensitive tumors to palbociclib plus ET. PFS analysis according to levels of mRNA PLK1 in patients treated with (**F**) palbociclib or (**G**) capecitabine. In PFS curves, Kaplan–Meier plots are used to represent the survival curves, while Cox models, adjusted by prognosis variables, are used to represent the values. LowExpr PLK1 (below median value); HighExpr PLK1 (above median value); median value = 8.380255. Sensitive: PFS in the upper quartile; Refractory: PFS in the lower quartile.

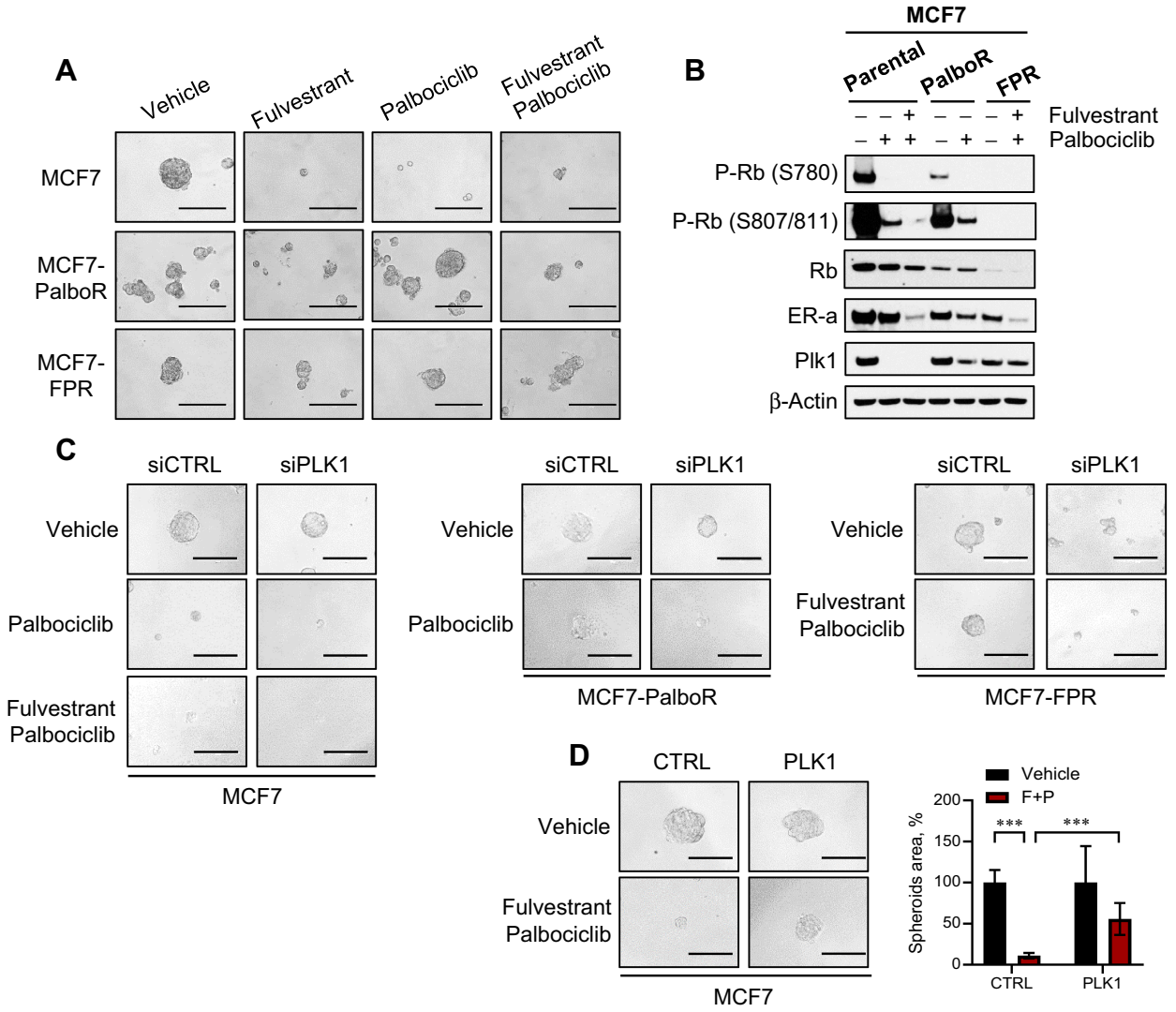

Figure 4.

Breast cancer cells resistant to palbociclib and ET depend on PLK1 expression for tumor growth. **A,** Representative images of breast tumor spheroids from MCF7, MCF7-PalboR (palbociclib resistant), or MCF7-FPR (fulvestrant-palbociclib–resistant) treated with the indicated drugs at 250 nmol/L final concentration, every 72 hours for 10 days. **B,** Western blot analysis for p-Rb (Ser780), p-Rb (Ser807/811), Rb, ER-α, Plk1 of whole cell lysates from MCF7 parental or resistant cells treated with vehicle, palbociclib alone, or in combination with fulvestrant at 1 μmol/L final concentration for 72 hours. β-Actin was used as a loading control. Images are representatives from three independent experiments. **C,** Representative images of breast tumor spheroids from MCF7, MCF7-PalboR, or MCF7-FPR transfected with 40 nmol/L siRNA scrambled (siCTRL) or siRNA versus PLK1 mRNA (siPLK1) for 48 hours and treated with vehicle (DMSO), 1 μmol/L of fulvestrant ± 1 μmol/L of palbociclib for another 6 days, every 72 hours. All images were captured at 20× magnification (bars = 200 μm). **D,** Representative images of breast tumor spheroids from MCF7-CTRL or PLK1-overexpressing cells treated for 6 days with 1 μmol/L fulvestrant + palbociclib. Images are representatives from three independent experiments. Spheroid area was calculated by ImageJ software and reported in the bar plot. Values were expressed as percentage relative to vehicle-treated controls. Data are expressed as mean ± SD of three separate experiments, indicated by error bars, performed in quadruplicate (***, $P < 0.001$, Student *t* test).

plus ET over capecitabine in terms of PFS. PFS subgroup analysis by stratification factors (visceral disease; sensitivity to prior ET; prior chemotherapy for MBC) also failed to show any difference in efficacy between palbociclib plus ET and capecitabine (9).

Three studies have previously evaluated, in *post hoc* analysis, the prognostic value of breast cancer intrinsic subtypes in HR+/HER2− MBC treated with ET and CDK4/6i. When evaluating this kind of studies, it is important to consider that intrinsic subtype can change between the primary tumor and the metastasis. Thus, LumA usually switch in metastatic sample either to LumB or HER2E subtype (14). Therefore, the prognostic/predictive performance of intrinsic subtype might differ among studies depending on the proportion of primary versus metastases samples analyzed.

Turner and colleagues (6), assessed the breast cancer intrinsic subtypes, using the HTG-AIMS classifier, in 302 tumor from the PALOMA-3 trial (53% from primary tumor samples), which studied fulvestrant with or without palbociclib in ET resistance MBC. The subtype distribution was LumA, 44.0%; LumB, 30.8%; HER2E, 20.9%; Normal-like, 2.6%; and Basal-like, 1.7%. LumA, LumB and non-luminal subtypes benefited from the addition of palbociclib to

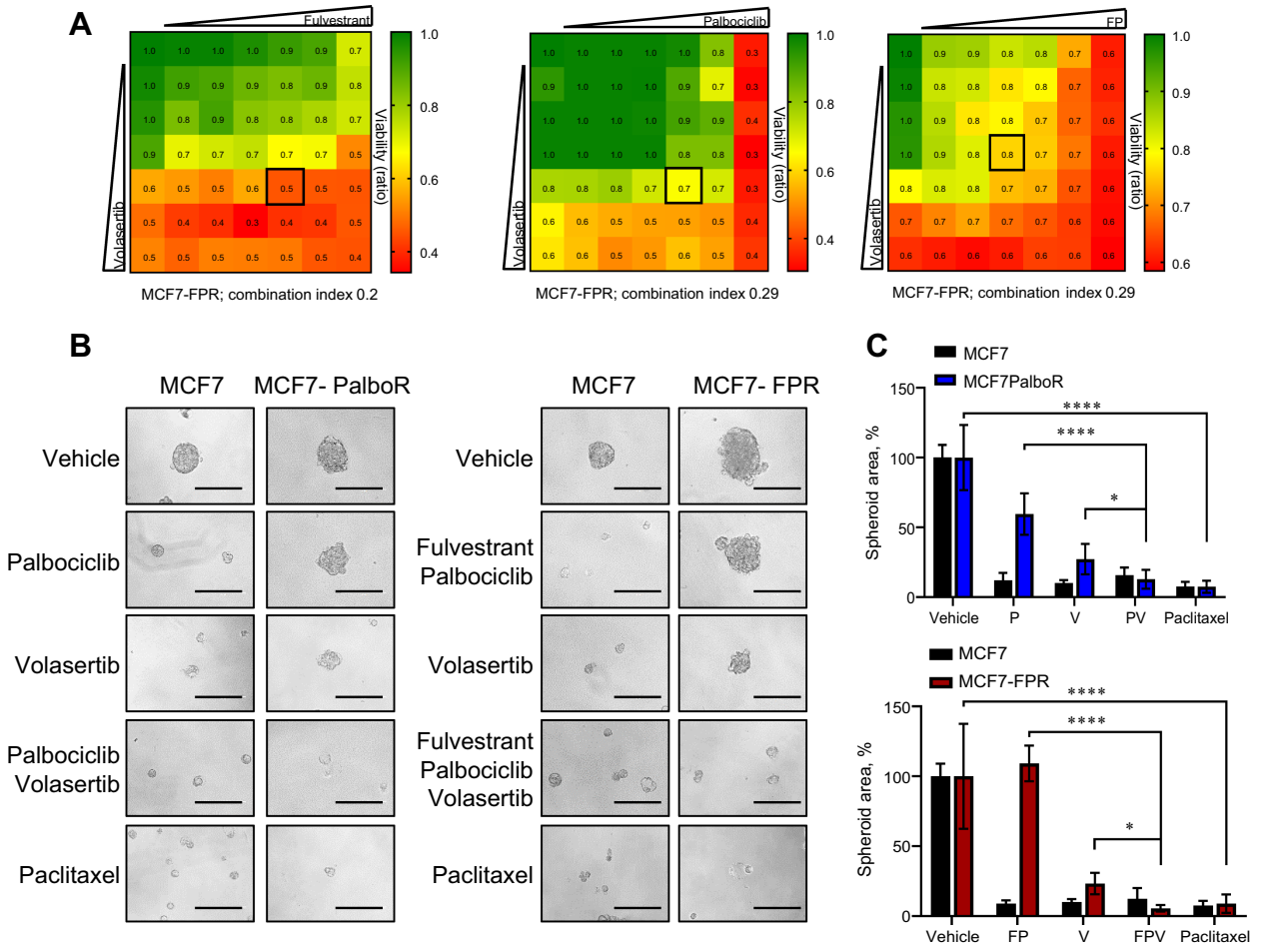

Figure 5.

Volasertib overcomes resistance to fulvestrant and palbociclib in MCF7, MCF7-PalboR, MCF7-FPR, and PLK1-overexpressing cells. **A,** Viability assay to assess pharmacologic synergy between fulvestrant-palbociclib and volasertib. MCF7-FPR were seeded in 96-well plates, treated with increasing concentrations of each drug alone or in combination (up to 1 mmol/L fulvestrant, 1 mmol/L palbociclib, 100 nmol/L volasertib) every 72 hours for 1 week. Cells were stained with crystal violet; staining intensities were quantified, and combination indexes were determined using the Chou-Talalay test by CompuSyn software. Numbers inside each box indicate the ratio of viable treated cells to untreated cells, from three independent experiments. **B,** Representative images of breast tumor spheroids from MCF7, MCF7-PalboR (left), or MCF7-FPR (right) treated with vehicle (DMSO), 500 nmol/L fulvestrant, 500 nmol/L palbociclib, 10 nmol/L volasertib, alone or combined, 10 nmol/L paclitaxel for 6 days, every 72 hours. All images were captured at 20× magnification (bars = 200 μm). **C,** Spheroid area was calculated by ImageJ software. Values were expressed as percentage relative to vehicle-treated controls. For all panels, data are expressed as mean ± SD of three separate experiments, indicated by error bars, performed in quadruplicate. Differences between data sets were determined by two-way ANOVA Bonferroni multiple comparisons (*, $P < 0.05$; ****, $P < 0.0001$).

fulvestrant, but LumA had the best absolute improvement in PFS compared with LumB and non-luminal subtypes. Finn and colleagues (7), assessed the breast cancer intrinsic subtypes using HTG-AIMS in 455 tumor samples (origin of tissue not recorded) from the PALOMA-2 trial, which studied letrozole with or without palbociclib as first-line treatment of HR+/HER2− MBC. The subtype distribution was LumA, 50.3%; LumB, 29.7%; HER2E, 18.7%; Normal-like, 0.9%; and Basal-like, 0.5%. Lum A and LumB subtypes benefited from the addition of palbociclib to letrozole, however the benefit of palbociclib in non-luminal subtypes was less than in Luminal subgroups. Prat and colleagues (8) reported the prognostic value of a customized PAM50 subtype classifier in 1,160 tumors (71% from primary tumor samples) included in 3 randomized trials evaluating ribociclib plus ET versus ET. The intrinsic subtype distribution was LumA, 46.7%; LumB, 24.0%; Normal-like, 14.0%; HER2E, 12.7%; and Basal-like, 2.6%. Ribociclib was associated with a significant PFS benefit across all subtypes, except the Basal-like subtype.

In our study, we observe a different subtype distribution than the studies reported above, probably because most of the tissue samples were derived from the archival primary tumor sample (72%). Thus, in our biomarker cohort HER2E subtype account for 6.5% of cases, while in PALOMA-3 trial, that is a similar study in terms of patient population, gene expression platform and methodology, but with 53% primary tumors analyzed, HER2E subtype was 21%. However, when we assessed AIMS-HTG intrinsic subtypes in metastatic samples, the proportion of HER2E subtype was 14%, similar to what is reported by Prat and colleagues (8) in metastases (16.8%).

Regarding outcome, our study reports median PFS for HER2E tumors of just 2.2 months with palbociclib plus ET in contrast to 9.2 months with capecitabine. This provides strong data to the

hypothesis that HER2E HR+/HER2− MBC might derive greater benefit from chemotherapy (such as capecitabine) than from CDK4/6i plus ET, which warrants confirmation in a clinical trial. However, although AIMS-HTG intrinsic subtypes are a strong prognostic factor in HR+/HER2− MBC, currently there is not any subtype-specific target that can be druggable. Experimentally, ER+/HER2− breast cancer cell lines only mirror some, but not all, the molecular properties of PAM50 intrinsic subtypes (15), which complicates the task of discovering molecular targets specific for each subtype. Increasing preclinical and clinical evidence support *CCNE1* expression as a marker of resistance to CDK4/6i (6, 16–19). High levels of CyclinE1 (protein encoded by *CCNE1*) in G1 can activate CDK2, hyperphosphorylated RB1 and drive G_1–S phase transition without requiring prior CDK4/6 activation, thus bypassing the action of CDK4/6i.

Our results provide further evidence to the role of *CCNE1* in driving resistance to CDK4/6i and identify capecitabine as an alternative option for these tumors. In agreement with previous report (6), the prediction power of *CCNE1* expression levels is greater when assayed over metastatic samples. In addition, *CCNE1* levels were higher in the 14 metastatic patients with paired primary and metastatic samples (**Fig. 2C** and **D**), suggesting that increased *CCNE1* expression might be an acquired mechanism of resistance, occurring during the tumor evolution, or due to ET pressure. Contrary to this role of *CCNE1* in driving resistance to CDK4/6i, recent studies (MONALEESA-3 study (fulvestrant ± ribociclib in AI resistant patients; ref. 20) and PALOMA-2 study (ref. 7; letrozole ± palbociclib)) reported a similar benefit from the addition of the CDK4/6i to ET, irrespective of *CCNE1* mRNA expression levels. This discordant data might be explained by several factors, including disease setting (first-line vs. second-line and beyond) and type of samples (metastasis versus primary) analyzed.

Our study also reveals that high levels of *PLK1* are strongly associated with resistance to palbociclib plus ET (i.e., fulvestrant or aromatase inhibitor) but not capecitabine. PLK1, a serine/threonine protein kinase, is a key regulator of completion of the G_2–M phase of the cell cycle. Previous studies have shown *PLK1* as a prognostic biomarker in early-stage breast cancer (21), a mechanism of acquired resistance to estrogen deprivation of ER+ breast cancer cell lines (13) and a therapeutic target in PDX models of advanced ER+ breast cancer resistant to palbociclib (22). Our *in vitro* studies, with two models of ER+ breast cancer showed that in parental cells, palbociclib or fulvestrant + palbociclib treatment induces a strong down-regulation of both PLK1 protein and mRNA levels. However, in models with acquired resistance to palbociclib plus fulvestrant, *PLK1* expression results unaltered upon pharmacologic treatment, in parallel to the higher levels of *PLK1* we observed in resistant tumors to palbociclib+ET in the biomarker study cohort. Furthermore, we have clearly shown that the genetic modulation of *PLK1* modifies the response to CDK4/6i treatment; thus, silencing *PLK1* in resistant cells reverses resistance to palbociclib plus fulvestrant, while in parental (sensitive cells) overexpression of *PLK1* increases resistance to palbociclib plus fulvestrant. Finally, we demonstrate that the pharmacologic inhibition of PLK1 with volasertib (a compound in clinical development) in combination with palbociclib completely abrogates resistance to palbociclib.

First-line combination of CDK4/6i plus ET is currently the best treatment option for most patients with HR+/HER2− MBC. According to our findings, tumors with high PLK1 are expected to progress early to CDK4/6i. After progression, although treatment with capecitabine or taxol is a reasonable option, responses to single-agent monotherapy are generally very poor, with median PFS of less than 3 months (23). In this context, evaluation of PLK1 inhibitors could be an effective strategy. PLK1 inhibitors monotherapy have limited clinical activity (24), however, strong synergistic effects have been observed for the combination of PLK1 inhibitors and taxanes. Different tumor type models, including breast cancer, show that PLK1 inhibitors synergize with taxanes specifically inhibiting the G_2–M transition, inducing mitotic arrest and apoptosis (25).

In summary, we confirm the association of non-luminal breast cancer subtype, and high levels of *CCNE1* with resistance to CDK4/6i, but not to capecitabine. We also found a strong association of high levels of *PLK1* and poor response to palbociclib. Finally, by *in vitro* studies, we showed that PLK1 inhibition overcomes resistance to CDK4/6i (i.e., palbociclib) in cell line models, supporting the clinical development of PLK1 inhibitors in HR+/HER2− MBC.

Authors' Disclosures

Á. Guerrero-Zotano reports grants, personal fees, and nonfinancial support from Pfizer; personal fees and nonfinancial support from Novartis; and personal fees from AstraZeneca, Menarini Stemline, Lilly, Exact Sciences, and Pierre Fabre during the conduct of the study. C. Zielinski reports grants from Eli Lilly, BMS, MSD, Novartis, Pfizer, AstraZeneca, and Servier during the conduct of the study; in addition, C. Zielinski has a patent for Hervaxx issued. M. Gil-Gil reports personal fees from Pfizer, Novartis, AstraZeneca, Daiichi-Sankyo, Gilead, Seagen, Roche, and Pierre Fabre during the conduct of the study. E.M. Ciruelos Gil reports personal fees from Pfizer, Novartis, AstraZeneca, Daiichi Sankyo, Lilly, Roche, and personal fees MSD outside the submitted work. J. Pascual reports grants from Boehringer-Ingelheim and personal fees from AstraZeneca and Daiichi Sankyo outside the submitted work. M. Muñoz-Mateu reports other support from Novartis, Roche, Eisai, Pierre Fabre, Seagen, Pfizer, Gilead, and Lilly outside the submitted work. B. Bermejo reports personal fees from Daiichi Sankyo, Novartis, and Lilly and other support from Pfizer outside the submitted work. M. Margeli Vila reports grants from Instituto de Salut Carlos III, InMaM project from "Plan Complementario de Biotecnología aplicada a la salud, financed by NextGenerationEU," and Pfizer (Pfizer, SA; Spain) and personal fees from Novartis, Pfizer, Lilly, Pierre Fabre, MSD, and Gilead outside the submitted work. A. Antón reports personal fees from Gilead, Eli Lilly, AstraZeneca/Daiichi Sankyo, Seagen, and Pfizer outside the submitted work. Y. Liu is employed by and holds shares in Pfizer. J.A. López-Guerrero reports grants from Generalitat Valenciana and European Commission and personal fees from AstraZeneca and Diaceutics outside the submitted work. N. Turner reports advisory board honoraria from AstraZeneca, Lilly, Pfizer, Roche/Genentech, Novartis, GlaxoSmithKline, Repare Therapeutics, Relay Therapeutics, Zentalis, Gilead, Inivata, Guardant, and Exact Sciences, and research funding from AstraZeneca, Pfizer, Roche/Genentech, Merck Sharpe and Dohme, Guardant Health, Invitae, Inivata, Personalis, and Natera. M. Martín reports other support from Pfizer and AstraZeneca during the conduct of the study as well as grants and personal fees from Roche/Genentech, Puma, and Novartis and personal fees from AstraZeneca, Amgen, Taiho Oncology, PharmaMar, Eli Lilly, Daiichi Sankyo, and Pfizer outside the submitted work. No disclosures were reported by the other authors.

Authors' Contributions

Á. Guerrero-Zotano: Conceptualization, resources, supervision, funding acquisition, validation, investigation, visualization, methodology, writing–original draft, project administration, writing–review and editing. **S. Belli:** Conceptualization, resources, data curation, formal analysis, supervision, validation, investigation, visualization, methodology, writing–original draft, project administration, writing–review and editing. **C. Zielinski:** Resources, investigation, writing–review and editing. **M. Gil-Gil:** Resources, investigation, writing–review and editing. **A. Fernandez-Serra:** Resources, data curation, validation, investigation, methodology, writing–review and editing. **M. Ruiz-Borrego:** Resources, investigation, writing–review and editing. **E.M. Ciruelos Gil:** Resources, investigation, writing–review and editing. **J. Pascual:** Conceptualization, visualization, methodology, writing–original draft, writing–review and

editing. **M. Muñoz-Mateu:** Resources, investigation, writing–review and editing. **B. Bermejo:** Resources, investigation, writing–review and editing. **M. Margeli Vila:** Resources, investigation, writing–review and editing. **A. Antón:** Resources, investigation, writing–review and editing. **L. Murillo:** Resources, investigation, writing–review and editing. **B. Nisenbaum:** Resources, investigation, writing–review and editing. **Y. Liu:** Resources, funding acquisition, writing–review and editing. **J. Herranz:** Resources, software, formal analysis, validation, visualization, methodology, writing–original draft, writing–review and editing. **D. Fernández-García:** Data curation, visualization, methodology, project administration, writing–review and editing. **R. Caballero:** Data curation, funding acquisition, visualization, methodology, writing–original draft, project administration, writing–review and editing. **J.A. López-Guerrero:** Resources, data curation, supervision, funding acquisition, validation, investigation, methodology, writing–review and editing. **R. Bianco:** Resources, data curation, supervision, funding acquisition, validation, investigation, methodology. **L. Formisano:** Conceptualization, resources, data curation, supervision, funding acquisition, validation, investigation, visualization, methodology, writing–original draft, project administration, writing–review and editing. **N. Turner:** Conceptualization, supervision, validation, visualization, methodology, writing–original draft, writing–review and editing. **M. Martín:** Conceptualization, resources, data curation, supervision, funding acquisition, validation, investigation, visualization, methodology, writing–original draft, project administration, writing–review and editing.

Acknowledgments

We thank all the patients included in this study and their families, as well as all the participating investigators and the support staff at each study site and at both the GEICAM and CECOG headquarters.

This work was supported by two funding companies: Pfizer Inc. (which provided palbociclib and exemestane through a collaboration agreement) and AstraZeneca (which provided fulvestrant). The trial sponsor is GEICAM Spanish Breast Cancer Group.

Preclinical experiments were performed at Department of Clinical Medicine and Surgery (University of Naples "Federico II") thanks to AIRC MFAG 21505 - 2018 grant (Prof. L. Formisano; S. Belli) and AIRC IG 21339 grant (Prof. R. Bianco).

The publication costs of this article were defrayed in part by the payment of publication fees. Therefore, and solely to indicate this fact, this article is hereby marked "advertisement" in accordance with 18 USC section 1734.

Note

Supplementary data for this article are available at Clinical Cancer Research Online (http://clincancerres.aacrjournals.org/).

Received July 18, 2022; revised October 10, 2022; accepted February 2, 2023; published first February 7, 2023.

References

1. Li J, Huo X, Zhao F, Ren D, Ahmad R, Yuan X, et al. Association of cyclin-dependent kinases 4 and 6 inhibitors with survival in patients with hormone receptor–positive metastatic breast cancer: a systematic review and meta-analysis. JAMA Network Open 2020;3:e2020312.
2. Gao JJ, Cheng J, Bloomquist E, Sanchez J, Wedam SB, Singh H, et al. CDK4/6 inhibitor treatment for patients with hormone receptor–positive, HER2-negative, advanced or metastatic breast cancer: a US food and drug administration pooled analysis. Lancet Oncol 2020;21:250–60.
3. Turner NC, Ro J, André F, Loi S, Verma S, Iwata H, et al. Palbociclib in hormone receptor–positive advanced breast cancer. N Engl J Med 2015;373:209–19.
4. Slamon DJ, Neven P, Chia S, Fasching PA, De Laurentiis M, Im S-A, et al. Phase III randomized study of ribociclib and fulvestrant in hormone receptor–positive, human epidermal growth factor receptor 2—negative advanced breast cancer: MONALEESA-3. J Clin Oncol 2018;36:2465–72.
5. Sledge GW, Toi M, Neven P, Sohn J, Inoue K, Pivot X, et al. MONARCH 2: abemaciclib in combination with fulvestrant in women with HR+/HER2-advanced breast cancer who had progressed while receiving endocrine therapy. J Clin Oncol 2017;35:2875–84.
6. Turner NC, Liu Y, Zhu Z, Loi S, Colleoni M, Loibl S, et al. Cyclin E1 expression and palbociclib efficacy in previously treated hormone receptor–positive metastatic breast cancer. J Clin Oncol 2019;37:1169–78.
7. Finn RS, Liu Y, Zhu Z, Martin M, Rugo HS, Diéras V, et al. Biomarker analyses of response to cyclin-dependent kinase 4/6 inhibition and endocrine therapy in women with treatment-naïve metastatic breast cancer. Clin Cancer Res 2020;26:110–21.
8. Prat A, Chaudhury A, Solovieff N, Paré L, Martinez D, Chic N, et al. Correlative biomarker analysis of intrinsic subtypes and efficacy across the MONALEESA phase III studies. J Clin Oncol 2021;39:1458–67.
9. Martin M, Zielinski C, Ruiz-Borrego M, Carrasco E, Turner N, Ciruelos EM, et al. Palbociclib in combination with endocrine therapy versus capecitabine in hormonal receptor–positive, human epidermal growth factor 2—negative, aromatase inhibitor-resistant metastatic breast cancer: a phase III randomized controlled trial-PEARL. Ann Oncol 2021;32:488–99.
10. Subramanian A, Tamayo P, Mootha VK, Mukherjee S, Ebert BL, Gillette MA, et al. Gene set enrichment analysis: a knowledge-based approach for interpreting genome-wide expression profiles. Proc Natl Acad Sci USA 2005;102:15545–50.
11. Rudolph D, Steegmaier M, Hoffmann M, Grauert M, Baum A, Quant J, et al. BI 6727, a Polo-like kinase inhibitor with improved pharmacokinetic profile and broad antitumor activity. Clin Cancer Res 2009;15:3094–102.
12. Chou TC. Drug combination studies and their synergy quantification using the Chou-Talalay method. Cancer Res 2010;70:440–6.
13. Bhola NE, Jansen VM, Bafna S, Giltnane JM, Balko JM, Estrada MV, et al. Kinome-wide functional screen identifies role of PLK1 in hormone-independent, ER-positive breast cancer. Cancer Res 2015;75:405–14.
14. Aftimos P, Oliveira M, Irrthum A, Fumagalli D, Sotiriou C, Gal-Yam EN, et al. Genomic and transcriptomic analyses of breast cancer primaries and matched metastases in AURORA, the Breast International Group (BIG) molecular screening initiative genomics and transcriptomics of metastatic breast cancer. Cancer Discov 2021;11:2796–811.
15. Jiang G, Zhang S, Yazdanparast A, Li M, Pawar AV, Liu Y, et al. Comprehensive comparison of molecular portraits between cell lines and tumors in breast cancer. BMC Genomics 2016;17:525.
16. Formisano L, Lu Y, Servetto A, Hanker AB, Jansen VM, Bauer JA, et al. Aberrant FGFR signaling mediates resistance to CDK4/6 inhibitors in ER+ breast cancer. Nat Commun 2019;10:1373.
17. Ma CX, Gao F, Luo J, Northfelt DW, Goetz M, Forero A, et al. NeoPalAna: Neoadjuvant palbociclib, a cyclin-dependent kinase 4/6 inhibitor, and anastrozole for clinical stage 2 or 3 estrogen receptor–positive breast cancer. Clin Cancer Res 2017;23:4055–65.
18. Hurvitz SA, Martin M, Press MF, Chan D, Fernandez-Abad M, Petru E, et al. Potent cell-cycle inhibition and upregulation of immune response with abemaciclib and anastrozole in neoMONARCH, phase II neoadjuvant study in HR(+)/HER2(-) breast cancer. Clin Cancer Res 2020;26:566–80.
19. Arnedos M, Bayar MA, Cheaib B, Scott V, Bouakka I, Valent A, et al. Modulation of Rb phosphorylation and antiproliferative response to palbociclib: the preoperative-palbociclib (POP) randomized clinical trial. Ann Oncol 2018;29:1755–62.
20. Chia S, Su F, Neven P, Im S-A, Petrakova K, Bianchi GV, et al. Abstract PD2–08: Gene expression analysis and association with treatment response in postmenopausal patients with hormone receptor–positive, HER2-negative advanced breast cancer in the MONALEESA-3 study. Cancer Res 2020;80:PD2–08–PD02–08.
21. Loddo M, Kingsbury SR, Rashid M, Proctor I, Holt C, Young J, et al. Cell-cycle-phase progression analysis identifies unique phenotypes of major prognostic and predictive significance in breast cancer. Br J Cancer 2009;100:959–70.
22. Montaudon E, Nikitorowicz-Buniak J, Sourd L, Morisset L, El Botty R, Huguet L, et al. PLK1 inhibition exhibits strong anti-tumoral activity in CCND1-driven breast cancer metastases with acquired palbociclib resistance. Nat Commun 2020;11:4053.
23. Rugo HS, Bardia A, Marmé F, Cortes J, Schmid P, Loirat D, et al. Sacituzumab govitecan in hormone receptor–positive/human epidermal growth factor receptor 2–negative metastatic breast cancer. J Clin Oncol 2022;40:3365–76.
24. Gutteridge REA, Ndiaye MA, Liu X, NJMct A. Plk1 inhibitors in cancer therapy: from laboratory to clinics. Mol Cancer Ther 2016;15:1427–35.
25. Chiappa M, Petrella S, Damia G, Broggini M, Guffanti F, Ricci F. Present and future perspective on PLK1 inhibition in cancer treatment. Front Oncol 2022;12:903016.